Control of Cell Adhesion by Mechanical Reinforcement of Soft Polyelectrolyte Films with Nanoparticles

ARTICLE *in* LANGMUIR · APRIL 2012

Impact Factor: 4.46 · DOI: 10.1021/la300635z · Source: PubMed

8 AUTHORS, INCLUDING:

Stephan Schmidt
Max Planck Institute of Colloids and Interfaces
52 PUBLICATIONS **767** CITATIONS
SEE PROFILE

Helmuth Moehwald
Max Planck Institute of Colloids and Interfaces
1,004 PUBLICATIONS **38,630** CITATIONS
SEE PROFILE

Dmitry Volodkin
Fraunhofer Institute for Biomedical Engineeri…
77 PUBLICATIONS **2,710** CITATIONS
SEE PROFILE

Langmuir

Article

pubs.acs.org/Langmuir

Control of Cell Adhesion by Mechanical Reinforcement of Soft Polyelectrolyte Films with Nanoparticles

Stephan Schmidt,[†,‡] Narayanan Madaboosi,[†,‡] Katja Uhlig,[†] Dorothee Köhler,[‡] André Skirtach,[‡,§,∥] Claus Duschl,[†] Helmuth Möhwald,[‡] and Dmitry V. Volodkin*[,†]

[†]Fraunhofer Institut für Biomedizinische Technik, Am Mühlenberg 13, 14476 Potsdam-Golm, Germany

[‡]Max Planck Institut für Kolloid und Grenzflächenforschung, Am Mühlenberg 1, 14476 Potsdam-Golm, Germany

[§]Department Molecular Biotechology, University of Ghent, Coupure Links 653, B-9000 Ghent, Belgium

[∥]Center for Nano- and Biophotonics, University of Ghent, Sint-Pietersnieuwstraat 41, B-9000 Ghent, Belgium

Supporting Information

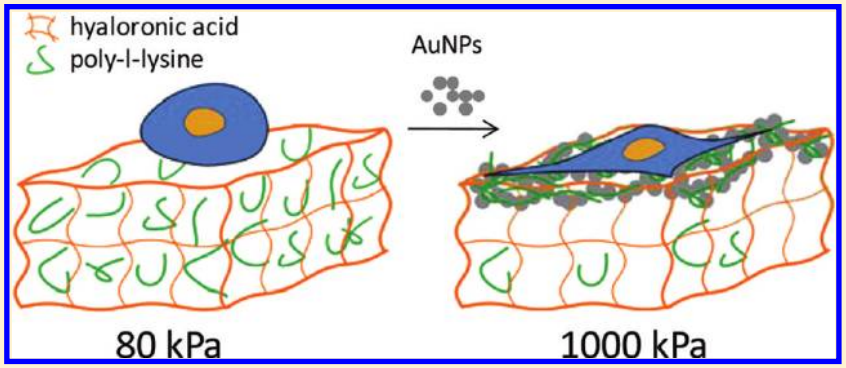

ABSTRACT: Chemical cross-linking is the standard approach to tune the mechanical properties of polymer coatings for cell culture applications. Here we show that the elastic modulus of highly swollen polyelectrolyte films composed of poly(L-lysine) (PLL) and hyaluronic acid (HA) can be changed by more than 1 order of magnitude by addition of gold nanoparticles (AuNPs) in a one-step procedure. This hydrogel-nanoparticle architecture has great potential as a platform for advanced cell engineering application, for example remote release of drugs. As a first step toward utilization of such films for biomedical applications we identify the most favorable polymer/nanoparticle composition for optimized cell adhesion on the films. Using atomic force microscopy (AFM) we determine the following surface parameters that are relevant for cell adhesion, i.e., stiffness, roughness, and protein interactions. Optimized cell adhesion is observed for films with an elastic modulus of about 1 MPa and a surface roughness on the order of 30 nm. The analysis further shows that AuNPs are not incorporated in the HA/PLL bulk but form clusters on the film surface. Combined studies of the elastic modulus and surface topography indicate a cluster percolation threshold at a critical surface coverage above which the film stiffness drastically increases. In this context we also discuss changes in film thickness, material density and swelling ratio due to nanoparticle treatment.

1. INTRODUCTION

There is a growing demand for surface coatings that allow not only the control of cellular adhesion but also the regulation of cell morphogenesis by surface mediated signaling or even remote release of drugs.[1−6] Control of the cell behavior can be achieved by adjusting chemical interactions between membrane and the synthetic surface.[7] There is also evidence that cellular signaling pathways and cell fate are affected by the mechanical environment of the cell.[8] It was found that a large range of cell parameters, such as adhesion, viability, proliferation, and motility can be controlled by the stiffness[9−11] and microscopic surface patterning[12] of the underlying film. Therefore, in view of biomedical applications, it is of great importance to be able to prepare coatings with well controlled topography and mechanical properties.

With the discovery of the layer-by-layer (LbL) deposition of polyelectrolyte multilayer films,[13,14] a versatile route toward thin films has been introduced. LbL assembly can be conducted with precise control over film properties such as thickness, microscopic roughness, and surface chemistry. More recent advances showed that specific biological activities can be induced by incorporation of bioactive species in polyelectrolyte multilayers.[5,6,15−21] For biomedical applications these materials are composed of biocompatible and degradable polyelectrolytes based on carbohydrates or poly(aminoacids). One of the most prominent polyelectrolyte pairs in this context is hyaluronic acid/poly(L-lysine) (HA/PLL), which was shown to form

Received: February 13, 2012
Revised: March 26, 2012
Published: April 17, 2012

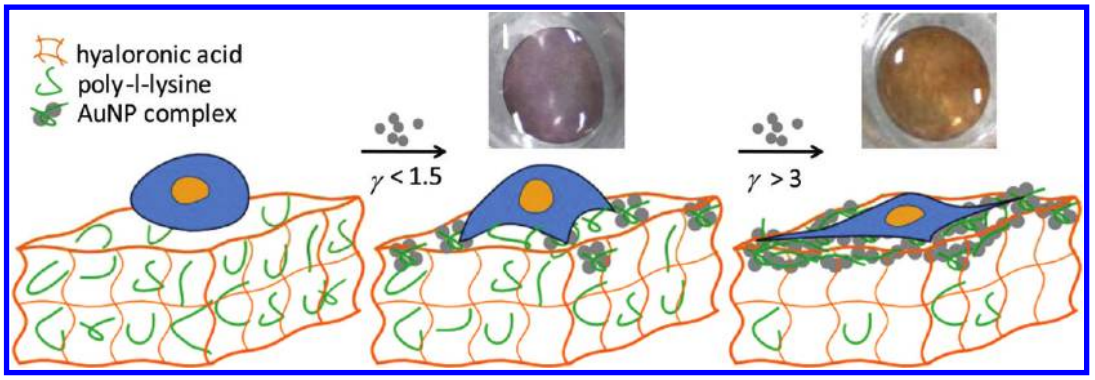

Figure 1. General scheme of the HA/PLL film structure; AuNPs (spheres) bind by complexation with PLL (in green) with the film. By addition of different amounts of AuNPs their surface concentration γ is increased. As a result, changes of the cellular adhesion can be expected as sketched. The top photographs show typical AuNPs modified films (γ = 1.5 and 4.5) on round coverslips (14 mm in diameter). Variation of γ leads to changes of the film color (top) due to shifts of the plasmon resonance frequency.

highly hydrated exponentially growing films.[22] Very useful features of these films is their ability to incorporate a large amount of active agents such as model dyes,[23] peptides,[24] nanoparticles,[25−27] and larger colloidal structures.[5,6,28−30] Biologically active species like DNA[5,6,31] or small drug molecules[32] have also been successfully incorporated in HA/PLL with the aim of direct manipulation of cellular behavior. As a prerequisite for these methods, cells need to be able to adhere and spread on the films. However, it was demonstrated that due to the low stiffness cell adhesion is generally not favored on native HA/PLL multilayers. Hence, the films have to be either capped with a stiffer polyelectrolyte multilayer[32] or chemically cross-linked[33−35] in order to allow for cell adhesion.

However, chemical cross-linking significantly reduces the polymer mobility in the film diminishing the ability to incorporate active species. Dense cross-linking also immobilizes biopolymers in the film and may disable their bioactivity.[36−38] Moreover, it can be expected that chemical cross-linking inhibits the biodegradation of the film.[39]

To overcome the problems associated with chemical cross-linking, we study the incorporation of nanoparticles into HA/PLL films as a means to adapt the material properties for optimized cell adhesion. This approach is inspired by a wealth of examples showing drastic improvement of mechanical properties by addition of various nanoscopic assemblies into polymers or gels.[40−42] Instead of end-capping the films via repeated polyelectrolyte deposition,[43] we suggest that a single nanoparticle absorption step could be sufficient to significantly change the mechanical properties of the film. To achieve this, we are going to mechanically reinforce the HA/PLL multilayers using negatively charged gold nanoparticles (AuNPs). Due to the large reservoir of PLL in the film,[5,27,44] one could expect complexation of a large amount of oppositely charged AuNPs such that a single deposition step may lead to drastic changes of the film properties. We evaluate the effect of a gradual increase of AuNP incorporation on cell adhesion and discuss material parameters that are relevant in this context, i.e., surface interaction energies, topography, and mechanical properties. The results will also shed light on the mechanisms of PLL complex formation in the film and the consequences of nanoparticle incorporation the overall film structure.

2. EXPERIMENTAL SECTION

2.1. Materials. Dried sodium hyaluronate (360 kDa) was obtained from Lifeforce Biomedical (U.S.A.). Hellmanex II solution was purchased from Hellma GmbH (Germany). PLL hydrobromide (24 kDa), polyethyleneimine (750 kDa), sodium chloride, Tris-Base, hydrochloric acid, and AuNPs (5 nm mean particle size, zeta potential −38 mV) were obtained from Sigma Aldrich (Germany). All chemicals were used as received.

2.2. Film Preparation. HA/PLL films were prepared as described elsewhere.[5] Briefly, after cleaning 14 mm round glass coversplips were immersed in aqueous solution of PEI (1 mg/mL) for 10 min followed by washing with buffer, then HA (0.5 mg/mL, in Tris buffer) for 10 min, followed by washing with buffer (10 mM Tris, 15 mM NaCl, pH 7.2−7.4). The glass substrate was consecutively immersed in aqueous solution of PLL (0.5 mg/mL, in Tris buffer) for 10 min followed by 3-fold washing with Tris buffer. After several washing steps, the glass slides were stored in buffer prior to AuNP deposition. AuNP modification of $(HA/PLL)_{24}$ films was performed by addition of 100, 300, 600, and 900 μL of aqueous AuNP solution with 3.45×10^{13} particles/mL onto LbL assembled films in a 24 well plate, resulting in 0.5−4.5 fold film surface coverage assuming the particles distribute homogeneously and form close packed layers on the surface. The solution was incubated overnight at room temperature for the adsorption of AuNPs, rinsed with Millipore water, and stored in buffer.

2.3. Atomic Force Microscopy. The measurements were performed on a "Nanowizard I" AFM (JPK Instruments AG, Berlin, Germany) in petridishes filled with the respective media (TRIS buffer or cell culture media). The AFM head is mounted on an optical microscope (IX51, Olympus, Japan). Using phase contrast optics (objective 63×/1.25 oil Ph3, Antiflex EC "Plan-Neofluar," Carl Zeiss AG, Germany) previously made scratches in the film can be identified and scanned to determine the film thickness. To collect elastic modulus data we mapped the surface by an array of AFM force−distance measurements on 3 different spots each 50 μm^2 grid with 8 × 8 data points. For this purpose we used uncoated silicon cantilevers (CSC 12, Mikromasch, Estonia) with a nominal spring constant of 0.2 N/m with silica probes (5 μm in diameter) attached to the apex of the cantilevers. The resulting force curves were evaluated using the Hertz−Sneddon force-defomation theory. To account for the finite thickness of the films on the hard glass support the Hertz−Sneddon relation was modified by a correction factor introduced by Dimitriadis et al.[45] Adhesion forces were determined by force mapping (8 × 8 pixels, 50 μm^2 grid), using silica particles as AFM probes (Microparticles GmbH, Berlin, Germany) with a diameter of 20 μm attached to tipless cantilevers (CSC 12 Mikromasch, Estonia), with a nominal spring constant of 0.2 N/m. Prior to the measurements the cantilevers and colloidal probes were rinsed with analytical grade isopropanol and water followed by treatment in air plasma at a pressure of 1 mbar for 2 min applying an intensity of 0.1 kW (PDC-32G plasma cleaner, Harrick, U.S.A.) followed by incubation in 10 μg/mL fibronectin (Sigma-Aldrich) in PBS for 1 h.

2.4. SEM and Film Thickness Measurements. The dried films on the glass coverslips were coated with a 5 nm gold film by vapor

dx.doi.org/10.1021/la300635z | Langmuir 2012, 28, 7249−7257

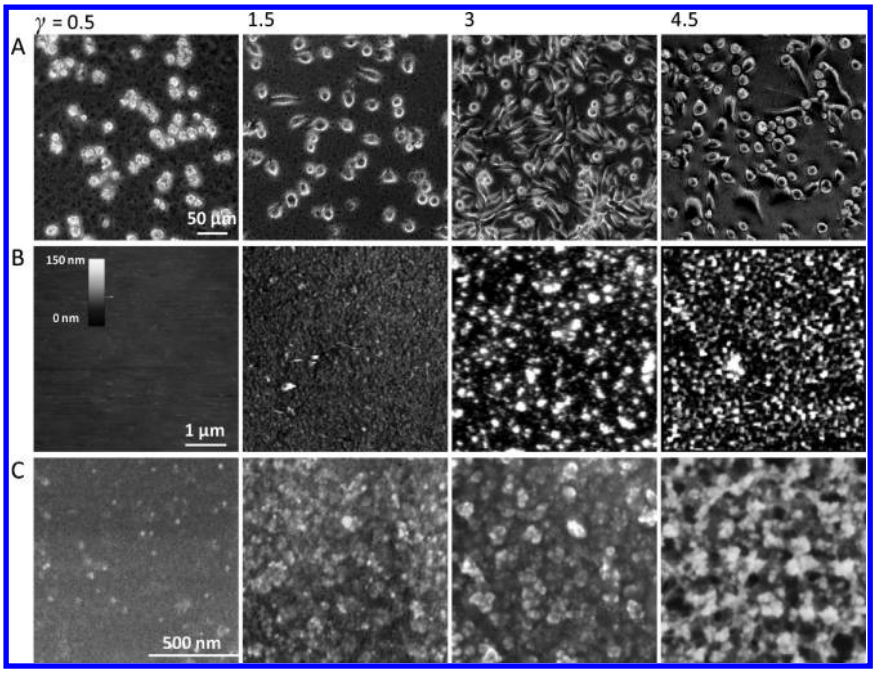

Figure 2. Overview of the cell adhesion behavior and the film surface morphology for different AuNP surface coverage γ. (A) Optical microscopy (phase contrast) of the cells on the films after incubation for five days; the cell adhesion is most pronounced for $\gamma = 3$. (B) AFM topography (height) images show the increase in surface roughness upon NP treatment. (C) Scanning electron micrographs indicate increase of the AuNP cluster size on the film surface increases as more AuNPs are added to the films. Additional images ($\gamma = 0$) are shown in the Supporting Information S1.

deposition and imaged via SEM. The film thickness was measured in buffer by first scratching the films with a small pipet tip and subsequent AFM height measurement of the scratched area.

2.5. Cell Assay. L929 mouse fibroblasts (ACC 2, DSMZ, Germany) were cultivated in DMEM medium containing 25 mM HEPES, 10% FCS, 2 mM L-glutamine, and 1% penicillin/streptomycin (all Biochrom, Germany). After seeding the cells (density), the cell medium was changed daily. After incubation on the films for 5 days at 37 °C and 5% CO_2 the cells were imaged in phase contrast mode using a 10 × 0.75 NA objective and a Nikon Digital Sight DS-L1 (Nikon, Germany). By alteration of the HA/PLL film the surface properties can be altered in favor of cell adhesion. We expect an increase in elastic modulus surface roughness as well as changes in the chemical interaction upon modification with AuNPs.

3. RESULTS AND DISCUSSION

3.1. Cell Adhesion and Spreading Correlates with the Gold Surface Coverage. We prepared HA/PLL films on the order of 2 μm in thickness on glass coverslips. The films were prepared by robot assisted deposition of 24 double deposition steps, resulting in a film with 24 bilayers $(HA/PLL)_{24}$, as described elsewhere.[29] The resulting native HA/PLL films are known for their cell repellent properties for many cell types.[35,46,47] Increasing the stiffness by means of chemical cross-linking generally improves the adhesion of cells.[35] Therefore, to a certain degree the cell repellent behavior is due to the low stiffness of native $(HA/PLL)_{24}$ films.[43] Here, instead of introducing chemical cross-links we aim at modification of the films by absorption of AuNPs, as schematically shown in Figure 1. Due to their negative surface charge (zeta potential −50 mV, as provided from manufacturer) we expect that the AuNPs (5 nm diameter) bind permanently by complex formation with the positively charged PLL chains in the films, similarly to biomolecules such as DNA.[5] The PLL molecules are mobile and can be recruited from the whole film volume to form complexes with charged species.[5,48] The AuNP treatment was conducted after depositing HA and PLL by adding a specific amount of AuNPs in suspension on the coverslips and incubating overnight. It can be assumed that all of the AuNPs are firmly bound with the film because extensive rinsing showed no changes in the UV−vis absorbance of the films. Also repeated AFM scanning in liquid showed no detachment of AuNPs due to possible shear forces. To describe the amount of added particles, we introduce an AuNP surface concentration (γ) of the films. We chose this notion because the following analysis suggested that the AuNP preferentially adhere at the films surface. The parameter γ is the ratio of the total surface required by the particles (assuming 2D close packing) and the available HA/PLL film surface on the coverslip. According to this definition the films prepared in this work had the following surface concentrations $\gamma = 0$, 0.5, 1.5, 3, and 4.5. Films with $\gamma < 1$ are not completely covered, films with $\gamma = 1$ present a (theoretical) monolayer of AuNPs at their surface, $\gamma > 1$ signifies a multilayer, assuming the particles distributed homogeneously, and only on the surface of the HA/PLL films. For example, a film with $\gamma = 3$ would have accumulated an amount of AuNPs that corresponds to three close packed AuNP monolayers. Please note, however, this notion only signifies the amount of AuNPs and should not imply that AuNPs form actual close packed layers, because the AuNPs do not assemble in a well ordered fashion, as depicted in Figure 1.

Further experiments were performed with L929 mouse fibroblasts, which were seeded on the films in cell culture medium and incubated for 5 d at a temperature of 37 °C. After incubation the cells were imaged using phase contrast optics; see Figure 2A. The fibroblasts did not spread on films with $\gamma = 0$ and 0.5%, whereas partial spreading is observed for $\gamma = 1.5$ and 4.5. The optimum spreading was observed at the intermediate surface concentration $\gamma = 3$. Larger amounts of

dx.doi.org/10.1021/la300635z | Langmuir 2012, 28, 7249−7257

AuNPs lead to less frequent cell adhesion (γ = 4.5) For γ > 10 the HA/PLL film becomes unstable (data not shown).

It is well-known that gold surfaces and thus also AuNPs layers may bind to cell adhesion controlling proteins and thus facilitate the adhesion of cells.[49,50] This may already explain the improved cell spreading for increasing γ. However, also bare films without AuNPs can be considered cell adhesive because they were terminated with PLL, a polymer that is well-known to strongly enhance cell adhesion due to complexation of membrane receptor binding proteins such as fibronectin.[51,52] Therefore, to understand the changes in cell behavior with γ, we first need to elucidate the cell−surface interactions for the different films. Here the film surface interactions were determined by measurement of adhesion energies via AFM colloidal probe. Strictly speaking, this method yields the work required to remove the colloidal probe from the film surface. Changes in adhesion energy with γ are very likely because the integration of negatively charged AuNPs supposedly alters the surface charge of the positively charged PLL/HA films. Indeed, films with AuNPs showed decreased adhesion energies when brought in contact with a negatively charged silica colloidal probe: In water the reduced electrostatic interactions led to vanishing adhesion energies on films with γ = 4.5 (0.2 ± 0.1 mJ/m^2), whereas attractive electrostatic and acid−base interactions between silica and PLL led to strong adhesions on bare HA/PLL films (11.2 ± 0.4 mJ/m^2, γ = 0).

Next, to mimic a cell−surface contact, we conducted AFM adhesion measurements with a fibronectin coated colloidal probe and in the complete culture medium. The adhesion energy of a fibronectin coated probe is a reasonable indicator for cell-surface interactions because fibroblasts secrete fibronectin to attach to their extracellular environment. Furthermore, the fact that it took the cells five days of incubation to reach optimum spreading indicates that fibronectin secretion precedes adhesion of the cells onto the films. To measure the interaction between the fibronectin coated probe and the film surfaces care was taken that the contact area between probe and film was identical for the different samples. The changes of the adhesion energy with surface coverage are shown in Figure 3. The work of adhesion between fibronectin and the films were larger for bare films without AuNPs (9.2 ± 0.4 mJ/m^2) and almost vanishing (0.4 ± 0.2 mJ/m^2) for surfaces with $\gamma \geq 3$, where the optimum cell adhesion was observed. The fact that the adhesion energy decreases with increasing γ is most likely a result of electrostatic interactions between fibronectin and the film. When adding the negatively charged AuNPs to the film, the positive surface charge due the terminating PLL layer is more and more compensated, i.e. for complete AuNP surface coverage the surface would be negatively charged. The AFM colloidal probe experiments were conducted at pH 7.4, thus fibronectin is negatively charged as well, therefore showing less adhesion with increasing γ.

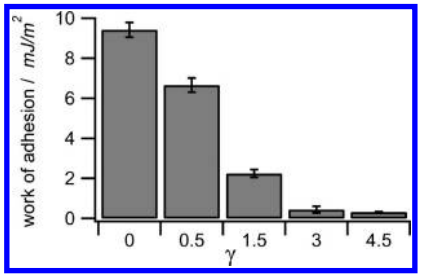

Figure 3. Work of adhesion between a fibronectin coated AFM colloidal probe and the AuNP modified HA/PLL films decreases with increasing AuNP coverage γ..

The fact that the interaction between the fibronectin coated probe and the film almost vanished in the presence of the AuNP coating suggests that cells bind less strongly to films with high AuNP coverage than to the native HA/PLL films. However, the cell experiment showed the opposite behavior. The fibroblasts did not adhere at all on the bare HA/PLL films, whereas spreading was pronounced for fibronectin repelling surfaces with γ > 1.5. Consequently, instead of surface interactions, changes in mechanical properties and surface morphology may have caused the pronounced spreading of the cells on surfaces with high NP coverage. These film parameters and the cellular response will be discussed in the next section.

3.2. AuNP Modification Drastically Affects Mechanical Properties and Film Morphology. Besides the observed variation in chemical interactions, we expect changes in mechanical properties of the film due to the AuNP treatment. Generally, by addition of AuNPs into a polymer network additional (physical) cross-links are introduced increasing the material stiffness. To quantify the changes in mechanical properties we measure the elastic modulus of the films by means of colloidal probe AFM. The data was gathered by force-mapping measurements on different position on the films elastic modulus value was determined from at least 100 force curves. Subsequent measurements on the same spot match reasonably well, indicating the film is not plastically deformed during the measurement. Note, that these films may behave not purely elastic upon deformation.[43] However, the films can be considered elastic for a force probe approach velocity of 1 μm/s that was applied here. The elastic response justifies the application of linear elasticity theory to evaluate the mechanical properties of the films. We defined 100 nm (∼10%) as upper sample deformation threshold. In this deformation range the force curves were fitted using the Hertz-Sneddon force-deformation theory modified by a correction factor[45] to account for the finite film thickness (see S4 for typical force curves and data fits). It should be noted that by this approach does not consider a possible vertical gradient of the elastic modulus because the AuNPs assemble in an inhomogeneous fashion at the surface of the film (see section 3.3). Therefore the mechanical analysis yields the effective modulus for the whole film. This modulus may sensitively depend on the size of the force probe and the applied force range. For our experiments we chose the colloidal probe approach to mimic a cell-surface contact and applied forces of a few nanonewtons, similar to the force range exerted by cells.

As expected, we obtained larger elastic moduli as γ increased; see Figure 4. The modulus increased 16-fold from 80 kPa for native HA/PLL films (γ = 0) to 1.3 MPa for film with the largest surface coverage (γ = 4.5). The modulus for films showing the best cell adhesion properties (γ = 3) was 0.9 MPa. Note, that the elastic moduli of the films increased after five days of cell growth when compared to the freshly prepared films. The increase was found to be stronger if the films contained less AuNPs: for γ = 0 the elastic modulus increased by 40% and for γ = 1.5 by 33%. The increase in the elastic modulus of higher AuNP loading was less than 10%, below the error of the measurement. This suggests that the PLL/HA films also took up cell secreted proteins or proteins in the cell media.

dx.doi.org/10.1021/la300635z | Langmuir 2012, 28, 7249−7257

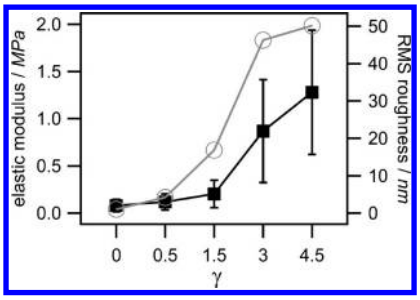

Figure 4. Elastic modulus (solid squares) and root-mean-square (rms, open circles) surface roughness increase monotonically with γ; the elastic modulus changes by more than 1 order of magnitude from 80 kPa (γ = 0) to 1.3 MPa (γ = 4.5); drastic changes occurred for γ > 1.5.

As a result the films became stiffer, in particular when the films contained low amounts of AuNPs. Nevertheless, the effect of AuNP treatment on the film stiffness is much larger than the changes due to protein adsorption.

The nanoscopic surface roughness is another important parameter controlling the adhesion between cells and substrate.[53,54] Consequently, we also studied the surface roughness in buffer as a function of γ. In this case the measurements were conducted by means of imaging AFM, as presented in Figure 2B. We found that the root-mean-square roughness (Figure 4) increased drastically from 1 nm for bare HA/PLL films (γ = 0) to 50 nm for film with maximum AuNP coverage (γ = 4.5). Note, however, due to the softness of the films and the resulting deformation induced by the AFM tip the actual roughness values might be larger. Nevertheless, also the SEM images suggest increases in surface roughness with increasing γ (Figure 2C).

Overall, the variation of the mechanical properties and surface roughness correlate with the changes in the cell adhesion. These are well-known phenomena, a number of studies showed that fibroblasts tend to adhere on surfaces with increased rigidity[55−57] and larger surface roughness.[53,58] Our results suggest that AuNP treated HA/PLL films promote cell adhesion in a similar fashion with the exception of samples with the largest AuNP concentration γ = 4.5. Here the cell adhesion was less pronounced as compared to γ = 3 although both stiffness and roughness were larger for γ = 4.5. This could be explained by the fact that fibroblast adhesion is not sensitive for changes of the elastic modulus in the MPa regime, as is the case for γ > 3. Moreover, very large AuNPs surface concentrations may prohibit access of the cell to the PLL contained within the film. Such interactions between cells and PLL may promote cell adhesion as indicated by the experiments with fibronectin coated colloidal probes. As a result, there is an optimum composition of the films at intermediate AuNP coverage ($\gamma \approx$ 3) that is characterized by high stiffness and roughness but also a certain PLL-mediated surface interaction with the cells.

3.3. Formation of AuNPs Clusters Roughens the Surfaces and Contributes to Film Stiffening. Reinforcement of rubbers or hydrogels by nanoparticle incorporation is due to the formation of additional (physical) cross-links in the network by which also the elastic modulus increases. Here the AFM measurements on the (HA/PLL)AuNP films revealed a 16-fold increase in elastic modulus, which seems exceptionally high considering that the NP volume ratio in the film ranged between only 0.08 and 1.9 vol % (see Supporting Information S2). Moreover, a drastic increase of the elastic modulus was observed by incorporation of only 0.8 vol % AuNPs (γ = 3, see Figure 4). Usually such a strong increase of the modulus is observed only above the nanoparticle percolation threshold, i.e., the point where the amount of randomly incorporated nanoparticles is sufficient to form a connected network throughout the film. The theoretical percolation threshold for spherical particles is reached only for volume ratios larger than 30%.[59] In reality the percolation threshold can be much lower (~2 vol %), e.g., for strong polymer−particle interactions.[42,60] However, even taking into account strong polymer−particle interactions does not explain the apparent percolation threshold as low as 0.8 vol %. This discrepancy could be explained by the fact that the particles did not distribute homogeneously in the bulk of the film as observed for other polyelectrolyte multilayers modified with stiff particles.[25,26] If the particles enrich at the surface of the film the percolation threshold would

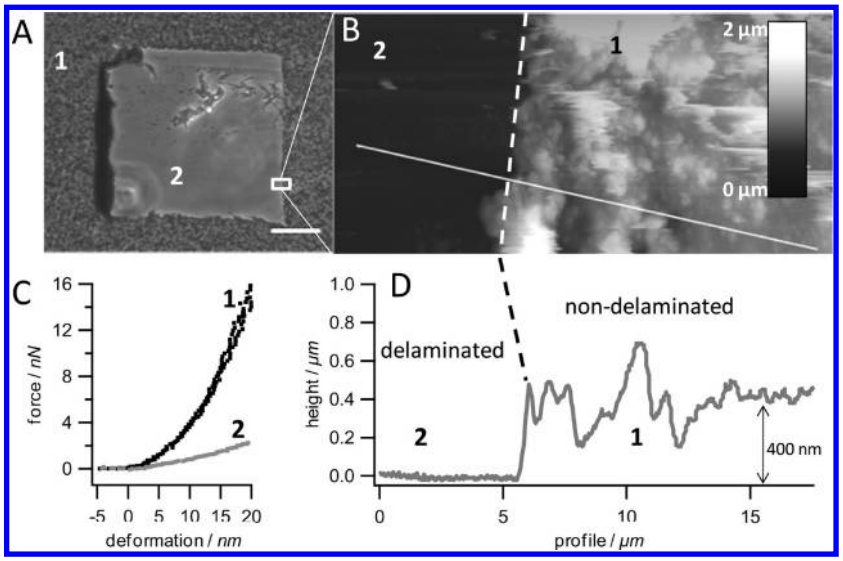

Figure 5. Delamination of the (HA/PLL)AuNPs films: (A) film with exposed sublayer at the center (phase contrast optics); (B) AFM image of the delaminated zone, the solid line highlights the profile measurement; (C) force curve on nondelaminated film surface (1) and within the delaminated zone (2) the respective elastic moduli were ~600 (1) and ~70 kPa (2); (D) the profile show that the delamination depth was 400 nm.

dx.doi.org/10.1021/la300635z | Langmuir 2012, 28, 7249−7257

be reached at the surface already for much lower (bulk) volume ratios.

To test this assumption, we analyzed the distribution of nanoparticles by delaminating a thin slice from HA/PLL-AuNP film (γ = 3) and probing the underlying film using AFM. The thin slice was removed by driving an AFM cantilever chip 400 nm into the film and moving the AFM stage laterally (see S5 for further explanations). Figure 5 shows the resulting delaminated film and presents AFM force deformation curves of the underlying layer (Figure 5C) and the height profile (Figure 5D) confirming that a 400 nm thick slice was removed from the surface. The elastic modulus calculated from AFM force deformation curves below the nondelaminated area (1) was similar to films with γ = 3, whereas the modulus of the delaminated surface (2) was similar the native HA/PLL film. Furthermore, the delaminated area possessed a much lower surface roughness as compared to the intact area. Taken together, the differences in elastic properties and surface roughness between the delaminated film and native films indicate that the AuNPs are present mainly at the surface of the HA/PLL multilayers.

The increase in roughness with higher γ as measured by AFM (Figure 4) already indicates that the AuNPs do not distribute homogeneously on the surface but form clusters of several hundred nanometers in diameter. Scanning electron microscopy further supports these findings and shows that the NP clusters increase in size when more AuNPs were added (Figure 2, panels B and C). The formation of clusters also explains why the particles were not able to enter the bulk of the film. As the negatively charged AuNPs are added to the films, they form complexes with PLL[5] before they can possibly diffuse deeper into the film. The complex formation with PLL leads to clusters of already about 20 nm in diameter even for the smallest added amount of AuNPs (γ = 0.5; see Figure 2C). The fact that these clusters appear at the surface of the film indicates they are already too large to travel further into the film. Addition of more AuNPs more likely leads to deposition of the particles at the film surface only. In this context, recent studies also showed that negatively charged silica particles (~1 μm in diameter) or AuNPs (20 nm in diameter) do not enter the bulk of the HA/PLL films and remain only partially incorporated at the film surface,[61] whereas they enter HA/PLL films which are not modified with nanoparticles.[62] Moreover, the large reservoir of PLL within the film enables complexation of more than a single monolayer of NPs (γ > 1), such that the cluster size exceeds 100 nm. This reservoir property has been identified in the pioneering studies on HA/PLL multilayers[22,48,63] and has been used for incorporation of DNA and other colloidal structures into the films.[5,6,29,31]

3.4. During AuNP Treatment the HA/PLL Films Shrink and Densify. In the previous section, we showed that the HA/PLL films were able to bind a large number of particles close to their surface, in our case up to 4.5 fold of a AuNP-monolayer. By simply stacking the 5 nm-sized AuNPs on top of each other, one would expect a thickness increase of about 20 nm in this case. However, measurements of the film thickness via AFM showed a gradual decrease of the film thickness with increasing AuNP surface coverage; see Figure 6. At the maximum AuNP surface coverage, the film thickness decreased to about half the thickness of the native $(HA/PLL)_{24}$ films. Remarkably, the film thicknesses of the respective dried films did not follow this trend. Here the thicknesses did not change regardless of the AuNP surface coverage. This indicates that the films do not

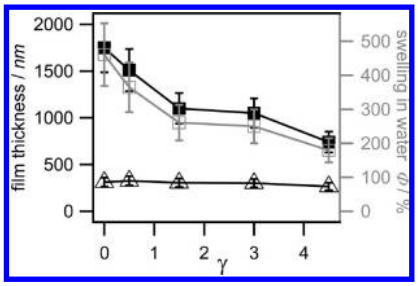

Figure 6. Changes of the film thickness in solution (solid squares), the dry film thickness (open triangles) and the swelling ratio (open squares) as a function of the AuNP surface concentration γ. A degree of swelling of 100% would indicate that the film thickness in water is twice the dry thickness. The thicknesses were determined by AFM height measurements of scratched film areas.

loose material but deswell as they are treated with the AuNPs. The question then is how the formation of a layer of AuNPs on the film surface can cause deswelling of the non-AuNP containing bulk of the film. Such deswelling could be caused by an osmotic effect upon AuNPs complexation with PLL: The driving force in polyelectrolyte complex formation is release of counterions due to ion pair formation.[64] In case of the HA/PLL films, the number of positive charges due to the PLL exceeds the number of negative charges of HA.[65] This is due to both, PLL termination of the film, and the fact that the charge density of PLL is larger as compared to HA. Therefore, it can be expected that a large number of chloride ions is present in the film to compensate for the excess of positive charges due to PLL. These chloride counterions contribute to the osmotic pressure of the film and are released upon complex formation between the negatively charged AuNPs and PLL. As a result, the osmotic pressure decreases and the film deswells upon addition of AuNPs. This is supported by the fact that about 13% of the total amount of PLL can be associated to the AuNPs in the films (Supporting Information S3).

Deswelling also implies a decrease in water content of the film. Here we represent the water content as a swelling ratio $\Phi = 100(t - t_d)/t_d$, where t is the thickness in solution and t_d is the dry-thickness. We find that the swelling ratio decreases from 460% (γ = 0) to 200% (γ = 4.5) as the AuNPs are added. Because water acts like a plasticizing agent for swollen hydrogels, this implies that the increase in elastic modulus due to AuNP coverage is not only due to additional cross-links in the film but also densification of the film and increase of the polymer content. The elastic modulus should be roughly proportional to the polymer content if we neglect physical cross-linking by AuNPs. From γ = 0 to 4.5 the film shrunk by a factor of 2 (in one dimension), meaning the volume of the film decreased by a factor of 2 as well, thus the polymer content increased a factor of 2. Therefore, the densification of the film due to deswelling would contribute only to a 2-fold increase of the elastic modulus, much lower than the observed 16-fold increase (Figure 4). Also, such a strong increase in elastic modulus by film densification was not observed in the delamination experiment wherein the film below the gold layer was probed (Figure 5). Additionally, comparison of Figures 2C and 6 shows that the sharp increase in modulus between γ = 1.5 and 3 does not correlate with changes of the swelling ratio. Overall, the results more likely indicate that the increase in the elastic modulus is due to incorporation of

dx.doi.org/10.1021/la300635z | Langmuir 2012, 28, 7249−7257

physical cross-links by AuNPs rather than densification of the multilayer.

4. CONCLUSION AND OUTLOOK

We have shown that the cell adhesion properties of highly swollen HA/PLL films can be improved by single step deposition of negatively charged AuNPs on the film surface. Comparative studies of the fibronectin surface interactions, elastic modulus, and surface topography via AFM were conducted to gain an insight into changes of material parameters relevant for cellular adhesion. The analysis indicated that the film stiffness and roughness increased due to AuNPs treatment which explains the improved cell adhesion.

The surface analysis also revealed that the HA/PLL films adsorb the nanoparticle in an unusual fashion. Deposition of charged particles on LbL assembled films consisting of highly charged polyelectrolytes typically leads to formation of a particle monolayer.[5,66] The monolayer usually saturates these films and prevents further nanoparticle adsorption. In case of highly swollen systems such as hydrogels or exponentially growing LbL films[25,26] also homogeneous particle distributions within the bulk of the film was reported. Here, as observed by SEM and AFM imaging, the AuNPs form multilayered clusters on the HA/PLL surface and do not penetrate into the bulk. This mode of particle adsorption allows the elastic modulus of the films to increase by a factor of 16 by just adding 0.8 vol % nanoparticles in a single adsorption step. Such sensitive changes of the elastic modulus could be explained by exceeding the AuNPs percolation threshold at the film surface, at which the surface can be considered completely "crosslinked" by nanoparticles.

Generally, single step nanoparticle deposition on HA/PLL films is not only much less elaborate than chemical cross-linking but also it is likely that mobility of polymers in the bulk of the film is preserved, as only the surface of the film is capped by nanoparticles. Therefore, such physically cross-linked nanoparticle assemblies allow not only for controlled mechanical reinforcement of the films and biodegradability but may also enable released of contained species by a mild external trigger, such as pH change. The observed buildup of particle clusters may also suggest that the film surface is not completely sealed by the particles supporting the release of contained molecules. Moreover, the modification of the film surface by light sensitive AuNPs offers the ability to remotely heat well-defined sites via laser irradiation in order to trigger release of active agents.[5,67]

Ongoing studies will address how the (HA/PLL)AuNP films can be used as a reservoir for biomolecules and how their release can be triggered. Also from a fundamental point of view the HA/PLL nanoparticle composite film opens many question that should be addressed in future studies. This concerns, for example, the densification of the film after nanoparticle loading and the possibility of reswelling the film by addition of PLL. Furthermore, it is of general interest to study how the cells probe the mechanical properties of composite films. For example, do they sense only the material surface or the effective modulus of the whole film? Due to the well-defined thickness of the whole film and the nanoparticle coating, the PLL/HA systems might offer new insights to such questions. Also the exact location and vertical structure of the nanoparticle layer on the film by microtome and cryo-SEM techniques will give further insight into the drastic changes of material properties due to nanoparticle adsorption. For cell cultivation applications possible direct interactions of the cells with the AuNP have to be analyzed to understand their role in cell adhesion and to test for a potential AuNP cell uptake. Other important parameters like degradability and complexation capacity, the effect of nanoparticle geometry and charge on mechanical reinforcement will be addressed as well.

■ ASSOCIATED CONTENT

Supporting Information

Additional micrographs of the films, AFM force-deformation curves, illustration of the delamination procedure, estimation of the amount of AuNPs in vol % in the HA/PLL films, and rough estimation of the amount of PLL bound to the AuNPs. This material is available free of charge via the Internet at http://pubs.acs.org.

■ AUTHOR INFORMATION

Corresponding Author

*Phone: +49-331-58187-327. Fax: +49-331-58187-399. E-mail: Dmitry.Volodkin@ibmt.fraunhofer.de.

Notes

The authors declare no competing financial interest.

■ ACKNOWLEDGMENTS

This work was supported by the Alexander von Humboldt-Foundation in the framework of the Sofja Kovalevskaja program.

■ REFERENCES

(1) von der Mark, K.; Park, J.; Bauer, S.; Schmuki, P. Nanoscale engineering of biomimetic surfaces: cues from the extracellular matrix. *Cell Tissue Res.* **2010**, *339*, 131−153.

(2) Alves, N. M.; Pashkuleva, I.; Reis, R. L.; Mano, J. F. Controlling Cell Behavior Through the Design of Polymer Surfaces. *Small* **2010**, *6*, 2208−2220.

(3) Lutolf, M. P. Integration column: Artificial ECM: expanding the cell biology toolbox in 3D. *Integr. Biol.* **2009**, *1*, 235−241.

(4) Rehfeldt, F.; Engler, A. J.; Eckhardt, A.; Ahmed, F.; Discher, D. E. Cell responses to the mechanochemical microenvironment--Implications for regenerative medicine and drug delivery. *Adv. Drug Delivery Rev.* **2007**, *59*, 1329−1339.

(5) Volodkin, D. V.; Madaboosi, N.; Blacklock, J.; Skirtach, A. G.; Mohwald, H. Surface-Supported Multilayers Decorated with Bio-active Material Aimed at Light-Triggered Drug Delivery. *Langmuir* **2009**, *25*, 14037−14043.

(6) Skirtach, A. G.; Volodkin, D. V.; Mohwald, H. Bio-interfaces-Interaction of PLL/HA Thick Films with Nanoparticles and Microcapsules. *ChemPhysChem* **2010**, *11*, 822−829.

(7) Dubiel, E. A.; Martin, Y.; Vermette, P. Bridging the Gap Between Physicochemistry and Interpretation Prevalent in Cell-Surface Interactions. *Chem. Rev.* **2011**, *111*, 2900−2936.

(8) Geiger, B.; Spatz, J. P.; Bershadsky, A. D. Environmental sensing through focal adhesions. *Nat. Rev. Mol. Cell Biol.* **2009**, *10*, 21−33.

(9) Discher, D. E.; Janmey, P.; Wang, Y. L. Tissue cells feel and respond to the stiffness of their substrate. *Science* **2005**, *310*, 1139−1143.

(10) Saha, K.; Keung, A. J.; Irwin, E. F.; Li, Y.; Little, L.; Schaffer, D. V.; Healy, K. E. Substrate Modulus Directs Neural Stem Cell Behavior. *Biophys. J.* **2008**, *95*, 4426−4438.

(11) Engler, A. J.; Sen, S.; Sweeney, H. L.; Discher, D. E. Matrix elasticity directs stem cell lineage specification. *Cell* **2006**, *126*, 677−689.

(12) Tay, C. Y.; Irvine, S. A.; Boey, F. Y. C.; Tan, L. P.; Venkatraman, S. Micro-/Nano-engineered Cellular Responses for Soft Tissue Engineering and Biomedical Applications. *Small* **2011**, *7*, 1361−1378.

(13) Decher, G.; Hong, J. D.; Schmitt, J. uildup of Ultrathin Multilayer Films by a Self-. Assembly Process 0.3. Consecutively Alternating Adsorption of Anionic and. Cationic Polyelectrolytes on Charged Surfaces. *Thin Solid Films* **1992**, *210*, 831−835.
(14) Decher, G. Fuzzy nanoassemblies: Toward layered polymeric multicomposites. *Science* **1997**, *277*, 1232−1237.
(15) Boudou, T.; Crouzier, T.; Ren, K. F.; Blin, G.; Picart, C. Multiple Functionalities of Polyelectrolyte Multilayer Films: New Biomedical Applications. *Adv. Mater.* **2010**, *22*, 441−467.
(16) Picart, C. Polyelectrolyte multilayer films: From physico-chemical properties to the control of cellular processes. *Curr. Med. Chem.* **2008**, *15*, 685−697.
(17) Rinaudo, M. Main properties and current applications of some polysaccharides as biomaterials. *Polym. Int.* **2008**, *57*, 397−430.
(18) Zelikin, A. N., Drug Releasing Polymer Thin Films: New Era of Surface-Mediated Drug Delivery. *ACS Nano* 4, 2494-2509.
(19) Jan, E.; Kotov, N. A. Successful Differentiation of Mouse Neural Stem Cells on Layer-by-Layer Assembled Single-Walled Carbon Nanotube Composite. *Nano Lett.* **2007**, *7*, 1123−1128.
(20) Kommireddy, D. S.; Sriram, S. M.; Lvov, Y. M.; Mills, D. K. Stem cell attachment to layer-by-layer assembled TiO2 nanoparticle thin films. *Biomaterials* **2006**, *27*, 4296−4303.
(21) Kommireddy, D. S.; Ichinose, I.; Lvov, Y. M.; Mills, D. K. Nanoparticle Multilayers: Surface Modification for Cell Attachment and Growth. *J. Biomed. Nanotechnol.* **2005**, *1*, 286−290.
(22) Picart, C.; Lavalle, P.; Hubert, P.; Cuisinier, F. J. G.; Decher, G.; Schaaf, P.; Voegel, J. C. Buildup mechanism for poly(L-lysine)/hyaluronic acid films onto a solid surface. *Langmuir* **2001**, *17*, 7414−7424.
(23) Sorrenti, E.; Ball, V.; Del Frari, D.; Arnoult, C.; Toniazzo, V.; Ruch, D., Incorporation of Copper (II) Phtalocyanines as Model Dyes in Exponentially Growing Polyelectrolyte Multilayer Films: A Multiparametric Investigation. *J. Phys. Chem. C 115*, 8248-8259.
(24) Wang, X. F.; Ji, J. Postdiffusion of Oligo-Peptide within Exponential Growth Multilayer Films for Localized Peptide Delivery. *Langmuir* **2009**, *25*, 11664−11671.
(25) Srivastava, S.; Podsiadlo, P.; Critchley, K.; Zhu, J.; Qin, M.; Shim, B. S.; Kotov, N. A. Single-Walled Carbon Nanotubes Spontaneous Loading into Exponentially Grown LBL Films. *Chem. Mater.* **2009**, *21*, 4397−4400.
(26) Srivastava, S.; Ball, V.; Podsiadlo, P.; Lee, J.; Ho, P.; Kotov, N. A. Reversible Loading and Unloading of Nanoparticles in â€œExponentiallyâ€ Growing Polyelectrolyte LBL Films. *J. Am. Chem. Soc.* **2008**, *130*, 3748−3749.
(27) Volodkin, D. V.; Delcea, M.; Moĥwald, H.; Skirtach, A. G. Remote Near-IR Light Activation of a Hyaluronic Acid/Poly(l-lysine) Multilayered Film and Film-Entrapped Microcapsules. *ACS Appl. Mater. Interfaces* **2009**, *1*, 1705−1710.
(28) Podsiadlo, P.; Michel, M.; Lee, J.; Verploegen, E.; Kam, N. W. S.; Ball, V.; Qi, Y.; Hart, A. J.; Hammond, P. T.; Kotov, N. A. Exponential growth of LBL films with incorporated inorganic sheets. *Nano Lett.* **2008**, *8*, 1762−1770.
(29) Volodkin, D.; Arntz, Y.; Schaaf, P.; Moehwald, H.; Voegel, J. C.; Ball, V. Composite multilayered biocompatible polyelectrolyte films with intact liposomes: stability and temperature triggered dye release. *Soft Matter* **2008**, *4*, 122−130.
(30) Volodkin, D. V.; Schaaf, P.; Mohwald, H.; Voegel, J. C.; Ball, V. Effective embedding of liposomes into polyelectrolyte multilayered films: the relative importance of lipid-polyelectrolyte and interpolyelectrolyte interactions. *Soft Matter* **2009**, *5*, 1394−1405.
(31) Zhang, X.; Sharma, K. K.; Boeglin, M.; Ogier, J.; Mainard, D.; Voegel, J. C.; Mely, Y.; Benkirane-Jessel, N. Transfection ability and intracellular DNA pathway of nanostructured gene-delivery systems. *Nano Lett.* **2008**, *8*, 2432−2436.
(32) Vodouhê, C.; Guen, E. L.; Garza, J. M.; Francius, G.; Déjugnat, C.; Ogier, J.; Schaaf, P.; Voegel, J.-C.; Lavalle, P. Control of drug accessibility on functional polyelectrolyte multilayer films. *Biomaterials* **2006**, *27*, 4149−4156.
(33) Schneider, A.; Francius, G.; Obeid, R.; Schwinte, P.; Hemmerle, J.; Frisch, B.; Schaaf, P.; Voegel, J. C.; Senger, B.; Picart, C. Polyelectrolyte multilayers with a tunable Young's modulus: Influence of film stiffness on cell adhesion. *Langmuir* **2006**, *22*, 1193−1200.
(34) Ren, K. F.; Fourel, L.; Rouviere, C. G.; Albiges-Rizo, C.; Picart, C., Manipulation of the adhesive behaviour of skeletal muscle cells on soft and stiff polyelectrolyte multilayers. *Acta Biomater. 6*, 4238-4248.
(35) Richert, L.; Boulmedais, F.; Lavalle, P.; Mutterer, J.; Ferreux, E.; Decher, G.; Schaaf, P.; Voegel, J. C.; Picart, C. Improvement of stability and cell adhesion properties of polyelectrolyte multilayer films by chemical cross-linking. *Biomacromolecules* **2004**, *5*, 284−294.
(36) Jessel, N.; Atalar, F.; Lavalle, P.; Mutterer, J.; Decher, G.; Schaaf, P.; Voegel, J. C.; Ogier, J. Bioactive Coatings Based on a Polyelectrolyte Multilayer Architecture Functionalized by Embedded Proteins. *Adv. Mater.* **2003**, *15*, 692−695.
(37) Thierry, B.; Winnik, F. o. M.; Merhi, Y.; Silver, J.; Tabrizian, M. Bioactive Coatings of Endovascular Stents Based on Polyelectrolyte Multilayers. *Biomacromolecules* **2003**, *4*, 1564−1571.
(38) Phelps, J. A.; Morisse, S.; Hindie, M.; Degat, M. C.; Pauthe, E.; Van Tassel, P. R., Nanofilm Biomaterials: Localized Cross-Linking To Optimize Mechanical Rigidity and Bioactivity. *Langmuir 27*, 1123-1130.
(39) Etienne, O.; Schneider, A.; Taddei, C.; Richert, L.; Schaaf, P.; Voegel, J.-C.; Egles, C.; Picart, C. Degradability of Polysaccharides Multilayer Films in the Oral Environment:â€‰ an in Vitro and in Vivo Study. *Biomacromolecules* **2005**, *6*, 726−733.
(40) Podsiadlo, P.; Kaushik, A. K.; Arruda, E. M.; Waas, A. M.; Shim, B. S.; Xu, J. D.; Nandivada, H.; Pumplin, B. G.; Lahann, J.; Ramamoorthy, A.; Kotov, N. A. Ultrastrong and stiff layered polymer nanocomposites. *Science* **2007**, *318*, 80−83.
(41) Fiedler, B.; Gojny, F. H.; Wichmann, M. H. G.; Nolte, M. C. M.; Schulte, K. Fundamental aspects of nano-reinforced composites. *Compos. Sci. Technol.* **2006**, *66*, 3115−3125.
(42) Zhang, Q.; Archer, L. A. Poly(ethylene oxide)/silica nanocomposites: Structure and rheology. *Langmuir* **2002**, *18*, 10435−10442.
(43) Francius, G.; Hemmerle, J.; Ball, V.; Lavalle, P.; Picart, C.; Voegel, J. C.; Schaaf, P.; Senger, B. Stiffening of soft polyelectrolyte architectures by multilayer capping evidenced by viscoelastic analysis of AFM indentation measurements. *J. Phys. Chem. C* **2007**, *111*, 8299−8306.
(44) Lavalle, P.; Picart, C.; Mutterer, J. r.; Gergely, C.; Reiss, H.; Voegel, J.-C.; Senger, B.; Schaaf, P. Modeling the Buildup of Polyelectrolyte Multilayer Films Having Exponential Growth. *J. Phys. Chem. B* **2003**, *108*, 635−648.
(45) Dimitriadis, E. K.; Horkay, F.; Maresca, J.; Kachar, B.; Chadwick, R. S. Determination of elastic moduli of thin layers of soft material using the atomic force microscope. *Biophys. J.* **2002**, *82*, 2798−2810.
(46) Richert, L.; Schneider, A.; Vautier, D.; Vodouhe, C.; Jessel, N.; Payan, E.; Schaaf, P.; Voegel, J. C.; Picart, C. Imaging cell interactions with native and crosslinked polyelectrolyte multilayers. *Cell Biochem. Biophys.* **2006**, *44*, 273−285.
(47) Semenov, O. V.; Malek, A.; Bittermann, A. G.; Voros, J.; Zisch, A. H. Engineered Polyelectrolyte Multilayer Substrates for Adhesion, Proliferation, and Differentiation of Human Mesenchymal Stem Cells. *Tissue Eng. Part A* **2009**, *15*, 2977−2990.
(48) Picart, C.; Mutterer, J.; Richert, L.; Luo, Y.; Prestwich, G. D.; Schaaf, P.; Voegel, J. C.; Lavalle, P. Molecular basis for the explanation of the exponential growth of polyelectrolyte multilayers. *Proc. Natl. Acad. Sci. U.S.A.* **2002**, *99*, 12531−12535.
(49) Lee, H.; Jang, Y.; Seo, J.; Nam, J. M.; Char, K. Nanoparticle-Functionalized Polymer Platform for Controlling Metastatic Cancer Cell Adhesion, Shape, and Motility. *ACS Nano* **2011**, *5*, 5444−5456.
(50) Coletti, D.; Scaramuzz, F. A.; Montemiglio, L. C.; Pristera, A.; Teodori, L.; Adamo, S.; Barteri, M. Culture of skeletal muscle cells in unprecedented proximity to a gold surface. *J. Biomed. Mater. Res. Part A* **2009**, *91A*, 370−377.

(51) Wittmer, C. R.; Phelps, J. A.; Saltzman, W. M.; Van Tassel, P. R. Fibronectin terminated multilayer films: Protein adsorption and cell attachment studies. *Biomaterials* **2007**, *28*, 851−860.
(52) Gentsch, R.; Pippig, F.; Schmidt, S.; Cernoch, P.; Polleux, J.; Borner, H. G., Single-Step Electrospinning to Bioactive Polymer Nanofibers. *Macromolecules 44*, 453-461.
(53) Karuri, N. W.; Liliensiek, S.; Teixeira, A. I.; Abrams, G.; Campbell, S.; Nealey, P. F.; Murphy, C. J. Biological length scale topography enhances cell-substratum adhesion of human corneal epithelial cells. *J. Cell Sci.* **2004**, *117*, 3153−3164.
(54) Brunetti, V.; Maiorano, G.; Rizzello, L.; Sorce, B.; Sabella, S.; Cingolani, R.; Pompa, P. P., Neurons sense nanoscale roughness with nanometer sensitivity. *Proc. Natl. Acad. Sci. U.S.A. 107*, 6264-6269.
(55) Lo, C. M.; Wang, H. B.; Dembo, M.; Wang, Y. L. Cell movement is guided by the rigidity of the substrate. *Biophys. J.* **2000**, *79*, 144−152.
(56) Pelham, R. J.; Wang, Y. L. Cell locomotion and focal adhesions are regulated by substrate flexibility. *Proc. Natl. Acad. Sci. U.S.A.* **1997**, *94*, 13661−13665.
(57) Schmidt, S.; Zeiser, M.; Hellweg, T.; Duschl, C.; Fery, A.; Mohwald, H. Adhesion and Mechanical Properties of PNIPAM Microgel Films and Their Potential Use as Switchable Cell Culture Substrates. *Adv. Funct. Mater.* **2010**, *20*, 3235−3243.
(58) Schulte, V. A.; Diìez, M.; Moìller, M.; Lensen, M. C. Surface Topography Induces Fibroblast Adhesion on Intrinsically Non-adhesive Poly(ethylene glycol) Substrates. *Biomacromolecules* **2009**, *10*, 2795−2801.
(59) Kirkpatrick, S. Percolation and Conduction. *Rev. Mod. Phys.* **1973**, *45*, 574.
(60) Yanagioka, M.; Frank, C. W. Defect Generation Surrounding Nanoparticles in a Cross-Linked Hydrogel Network. *Langmuir* **2009**, *25*, 5927−5939.
(61) Kohler, D.; Madaboosi, N.; Delcea, M.; Schmidt, S.; De Geest, B. G.; Volodkin, D. V.; Möhwald, H.; Skirtach, A. G. Patchiness of Embedded Particles and Film Stiffness Control Through Concentration of Gold Nanoparticles. *Adv. Mater.* **2012**, *24*, 1095−1100.
(62) Delcea, M.; Madaboosi, N.; Yashchenok, A. M.; Subedi, P.; Volodkin, D. V.; De Geest, B. G.; Mohwald, H.; Skirtach, A. G. Anisotropic multicompartment micro- and nano-capsules produced via embedding into biocompatible PLL/HA films. *Chem. Commun.* **2011**, *47*, 2098−2100.
(63) Garza, J. M. n.; Schaaf, P.; Muller, S.; Ball, V.; Stoltz, J.-F. o.; Voegel, J.-C.; Lavalle, P. Multicompartment Films Made of Alternate Polyelectrolyte Multilayers of Exponential and Linear Growth. *Langmuir* **2004**, *20*, 7298−7302.
(64) v. Klitzing, R. Internal structure of polyelectrolyte multilayer assemblies. *Phys. Chem. Chem. Phys.* **2006**, *8*, 5012−5033.
(65) Crouzier, T.; Picart, C. Ion Pairing and Hydration in Polyelectrolyte Multilayer Films Containing Polysaccharides. *Biomacromolecules* **2009**, *10*, 433−442.
(66) Hicks, J. F.; Seok-Shon, Y.; Murray, R. W. Layer-by-layer growth of polymer/nanoparticle films containing monolayer-protected gold clusters. *Langmuir* **2002**, *18*, 2288−2294.
(67) Skirtach, A. G.; Dejugnat, C.; Braun, D.; Susha, A. S.; Rogach, A. L.; Parak, W. J.; Mohwald, H.; Sukhorukov, G. B. The role of metal nanoparticles in remote release of encapsulated materials. *Nano Lett.* **2005**, *5*, 1371−1377.